REPORT DOCUMENTATION PAGE

Form Approved
OMB No. 0704-0188

1. REPORT DATE *(DD-MM-YYYY)*	**2. REPORT TYPE**	**3. DATES COVERED** *(From - To)*
June 2014	Technical Paper	June 2014- July 2014

4. TITLE AND SUBTITLE

Near-Wall Velocity Field Measurements of a Very Low Momentum Flux Transverse Jet

5a. CONTRACT NUMBER
FA9300-12-C-0002

5b. GRANT NUMBER

5c. PROGRAM ELEMENT NUMBER

6. AUTHOR(S)

Salazar, Forliti, Kuzmich, Coy

5d. PROJECT NUMBER

5e. TASK NUMBER

5f. WORK UNIT NUMBER
Q09Z

7. PERFORMING ORGANIZATION NAME(S) AND ADDRESS(ES)

Air Force Research Laboratory (AFMC)
AFRL/RQRC
10 E. Saturn Blvd.
Edwards AFB CA 93524-7680

8. PERFORMING ORGANIZATION REPORT NO.

9. SPONSORING / MONITORING AGENCY NAME(S) AND ADDRESS(ES)

Air Force Research Laboratory (AFMC)
AFRL/RQR
5 Pollux Drive
Edwards AFB CA 93524-7048

10. SPONSOR/MONITOR'S ACRONYM(S)

11. SPONSOR/MONITOR'S REPORT NUMBER(S)
AFRL-RQ-ED-TP-2014-177

12. DISTRIBUTION / AVAILABILITY STATEMENT
Distribution A: Approved for Public Release; Distribution Unlimited

13. SUPPLEMENTARY NOTES
Technical paper presented at 50th AIAA/ASME/SAE/ASEE Joint Propulsion Conference, Cleveland, OH, 28-30 July, 2014.
PA#14344

14. ABSTRACT

Transverse jets have been the subject of study for several decades due to their relevance in a number of flows in nature and engineering applications. The momentum flux ratio between the jet and crossflow is generally considered to be the leading independent parameter, and has been explored extensively over a nominal range from unity to several hundred. The current study considers the flow field of a transverse jet at momentum flux ratios much smaller than unity. A modulated absorption/emission thermometry technique under development at AFRL requires a narrow film barrier to maintain a clean optical access window, while limiting the transverse penetration of the jet into the crossflow to avoid corruption of the optical measurement. The current effort examined the near field behavior of very low momentum flux ratio transverse jets to elucidate the jet and crossflow interactions. Under low momentum flux ratio conditions, the crossflow has sufficient local momentum near the injection location, exceeding that of the jet, which leads to crossflow ingestion. It was expected that reduced area and consequent increase in mean jet velocity would increase the effective momentum flux ratio which would lead to increased momentum flux and penetration into the crossflow. However, the complex 3-dimensional interaction between the jet and crossflow suggests penetration is far reduced for these very low momentum flux ratio cases. Particle image velocimetry was used to investigate the jet and cross flow interactions near the jet exit over a range of low momentum flux ratios, $0.0013 \leq J \leq 0.075$. A fully developed laminar jet was injected into a fully developed turbulent channel crossflow. The two lowest momentum flux ratio cases were found to penetrate the least into the crossflow with regard to mean behavior of the jet. However, these same cases were found to have the highest levels of unsteadiness including a pulse-like behavior which created localized regions of increased velocity nearly $1.5Dj$ into the crossflow. These results help tailor the specific film flow requirement for the MAET technique under development at AFRL.

15. SUBJECT TERMS

16. SECURITY CLASSIFICATION OF:			**17. LIMITATION OF ABSTRACT**	**18. NUMBER OF PAGES**	**19a. NAME OF RESPONSIBLE PERSON**
					Nils Sedano
a. REPORT	**b. ABSTRACT**	**c. THIS PAGE**	SAR	24	**19b. TELEPHONE NO** *(include area code)*
Unclassified	**Unclassified**	**Unclassified**			661-275-5972

Standard Form 298 (Rev. 8-98)
Prescribed by ANSI Std. 239.18

Near-Wall Velocity Field Measurements of a Very Low Momentum Flux Transverse Jet

Salazar, D. V. and Forliti, D. J.

Sierra Lobo, Inc., Edwards AFB, CA, 93524

Kuzmich, K. and Coy, E.

Air Force Research Laboratory (RQRC), Edwards AFB, CA, 93524

Abstract

Transverse jets have been the subject of study for several decades due to their relevance in a number of flows in nature and engineering applications. The momentum flux ratio between the jet and crossflow is generally considered to be the leading independent parameter, and has been explored extensively over a nominal range from unity to several hundred. The current study considers the flow field of a transverse jet at momentum flux ratios much smaller than unity. A modulated absorption/emission thermometry technique under development at AFRL requires a narrow film barrier to maintain a clean optical access window, while limiting the transverse penetration of the jet into the crossflow to avoid corruption of the optical measurement. The current effort examined the near field behavior of very low momentum flux ratio transverse jets to elucidate the jet and crossflow interactions. Under low momentum flux ratio conditions, the crossflow has sufficient local momentum near the injection location, exceeding that of the jet, which leads to crossflow ingestion. It was expected that reduced area and consequent increase in mean jet velocity would increase the effective momentum flux ratio which would lead to increased momentum flux and penetration into the crossflow. However, the complex 3-dimensional interaction between the jet and crossflow suggests penetration is far reduced for these very low momentum flux ratio cases. Particle image velocimetry was used to investigate

the jet and cross flow interactions near the jet exit over a range of low momentum flux ratios, $0.0013 \leq J \leq 0.075$. A fully developed laminar jet was injected into a fully developed turbulent channel crossflow. The two lowest momentum flux ratio cases were found to penetrate the least into the crossflow with regard to mean behavior of the jet. However, these same cases were found to have the highest levels of unsteadiness including a pulse-like behavior which created localized regions of increased velocity nearly $1.5D_j$ into the crossflow. These results help tailor the specific film flow requirement for the MAET technique under development at AFRL.

Nomenclature

D_j = jet diameter

f = frequency

h = height

h_c = channel height

J = momentum flux ratio

l = length

M = blowing ratio

Q = cross-correlation peak ratio

u = streamwise velocity

$\overline{u_J}$ = mean jet velocity

$\overline{u_o}$ = mean crossflow velocity

$\overline{u'v'}$ = Reynolds shear stress

v = transverse velocity

w = width

y_p = jet penetration length

ρ = density

ω = vorticity

I. Introduction

Non-intrusive optical diagnostics play a critical role in experimental thermal science research. They offer unique insight and access to information without dramatically altering experimental conditions. Optical diagnostics eliminate the need to expose instrumentation to the highly corrosive environments typical of liquid rocket engines (LRE). However, soot and moisture formation on optical access windows make it difficult to access areas of interest in LRE systems using line of sight diagnostics. Consequently, the availability of reliable optical diagnostics which can be implemented on LRE and related experiments remains limited.

Although modulated absorption-emission thermometry (MAET) has been developed in the past for making soot volume fraction and soot temperature measurements in flames,[1,2] the Air Force Research Laboratory (AFRL) at Edwards Air Force Base has developed an MAET technique for making mean channel-temperature measurements in supercritical combustion environments.[3]

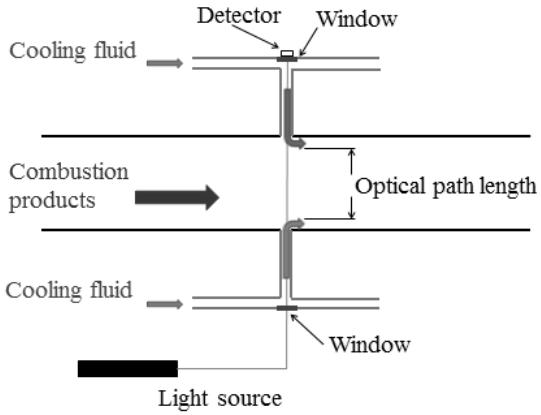

Figure 1. MAET optical setup.

Difficulties in obtaining accurate measurements with MAET persist. Specifically, knowledge of the optical path length used to calculate mean temperature is critical for minimizing uncertainty. Fig. 1 illustrates the optical setup of an experiment at AFRL which implements MAET. This technique implements transverse jets as transparent optical barriers to eliminate soot and moisture formation on optical access windows. Due to the fact that the jets penetrate into the crossflow, the penetration length will vary with momentum flux ratio. The momentum flux ratio $J = \rho_j \overline{u_j}^2 / \rho_o \overline{u_o}^2$ is defined as the momentum flux of the jet divided by that of the crossflow, where ρ is density, u is streamwise velocity, and the subscripts j and o represent the jet and crossflow, respectively.

Although, transverse jets have been studied extensively in recent decades,[4-14] the majority of jet in crossflow (JICF) studies focus on momentum flux ratios greater than unity. Film cooling research investigates J values much closer to the range of interest to the present study.[15-18] Whereas film cooling research focuses on minimizing penetration to reduce heat transfer to the crossflow, the goal of the present study is to minimize penetration to limit the difference between the optical path length and the channel height.

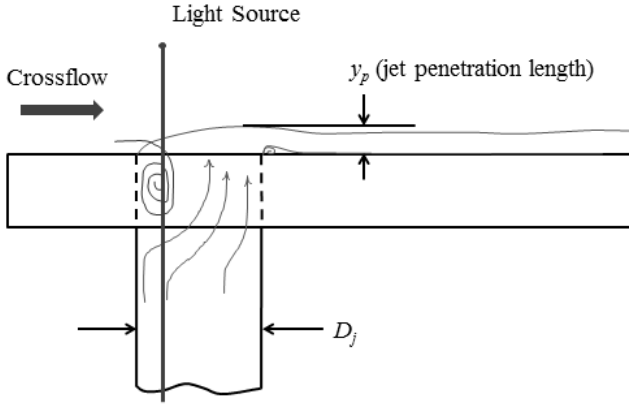

Figure 2. In-hole jet and crossflow fluid interaction.

As illustrated in Fig. 2, the complex interaction between the low momentum flux transverse jet and the higher momentum flux crossflow makes it difficult to predict the extent to which the jet penetrates into the crossflow and where the jet fluid exists within the jet hole. Ingestion of crossflow fluid further complicates the light-source path due to the existence of both crossflow and jet fluid in the jet hole. Although previous studies have shown a highly three-dimensional interaction for low momentum flux jets,[18,19] the present study focuses on characterizing the jet's two-dimensional behavior at the centerline since that is where the jet was expected to penetrate the furthest into the crossflow.

In terms of blowing ratio, Bidan and Nikitopoulos[19] show that for values below $M < 0.275$, the jet remains attached to the wall on the downstream side of the jet, thus minimizing penetration into the crossflow. Blowing ratio $M = \sqrt{\rho_j \overline{u_j}^2 / \rho_o \overline{u_o}^2}$ is defined as the square root of *J*. The present study verifies this behavior and explores the jet and crossflow interaction in a much lower range $0.036 \leq M \leq 0.27$. This very low range of *M*, and the corresponding values of *J*, has not been addressed in the research literature. This is the motivation for the present study. Although film cooling research has found *M* relevant in studying transverse jets, the focus in this study is on *J*, due to its relevance in the MAET technique being developed at AFRL. Characterization of the jet and crossflow interaction in this range of momentum flux ratios, $0.0013 \leq J \leq 0.075$, allows the penetration depth of the jet into the crossflow to be optimized to obtain the optical path length needed to calculate the mean temperature across the square channel of the MAET system illustrated in Fig. 1 and minimizes the effects of jet fluid in the crossflow.

II. Experimental Methods

The experimental setup and cross-section of the test section are shown in Fig. 3. A Gast Regenair® regenerative blower was used to generate the crossflow. The air flows through a plenum, a honeycomb flow straightener, through a perforated plate, and into the test section. The length, width, and height of the plenum are 910, 580, and 580 mm, respectively, and the length-to-diameter ratio of the honeycomb channels is l/D = 31. The test section consists of cast acrylic sheets fitted into a rectangular channel with a length-to-height ratio of l/h = 40.5 and an aspect ratio of w/h = 4. The center of the jet is located at thirty-seven channel heights, l/h_c = 37, downstream of the perforated plate. This allows for fully developed channel flow to be achieved at the point of injection. Fig. 4 contains the velocity profile of the crossflow normalized by the mean, $\bar{u}_o$ = 2.71 m/s. This mean is calculated from the crossflow velocity profile at the centerline of the channel, z = 0, approximately one channel height, h_c,, upstream of the jet. The Reynolds number of the crossflow using the hydraulic diameter of the jet, D_h = 76.2 mm, is Re_o = 14,000.

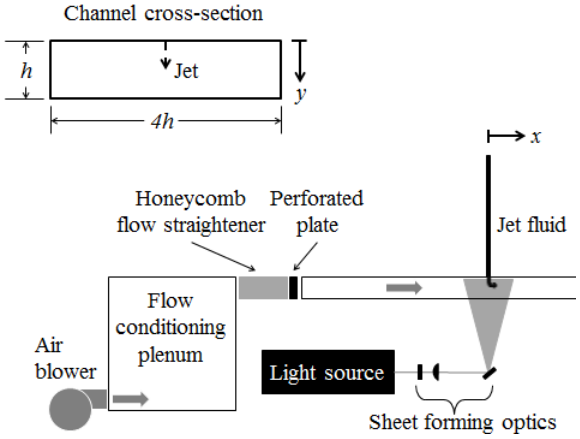

Figure 3. PIV experimental setup and test section.

Jet fluid is supplied to the test section through a high-pressure supply of nitrogen gas. A needle valve upstream of the jet tube is used to regulate the flow to the test section. The jet tube consists of a steel pipe which provides a length-to-jet diameter ratio of l/D_j = 94. This provides fully developed pipe flow at the jet exit. Fig. 4 contains the velocity profile of the jet normalized

by the mean, $\bar{u}_j$ = 0.731 m/s. This mean is calculated from the jet exit velocity profile at the centerline of the jet, without crossflow, approximately 0.5 mm from the near wall. The jet exit velocity profile in Fig. 4 corresponds to J = 0.075. Velocity profiles for all other cases exhibit the same trend. The jet Reynolds number for the various J values studied ranges between $62 \leq Re_j \leq 472$. Two sets of data were taken for each momentum flux ratio case, one of the jet only (without crossflow), and one of the jet and crossflow. 500 and 3,000 images were taken for each set, respectively. A time average of image pairs for both sets of tests was conducted. 500 and 3,000 images minimized the number of images that needed to be processed, respectively, thus capturing the mean behavior of the jet and interaction in 0.90 s.

A Laskin nozzle was used to generate olive oil droplets approximately 1 μm in diameter with approximately 20 particles per 32 x 32 px interrogation region. Particle seeding of the flows occurs immediately downstream of the blower and upstream of the needle valve for the mainflow and jet, respectively.

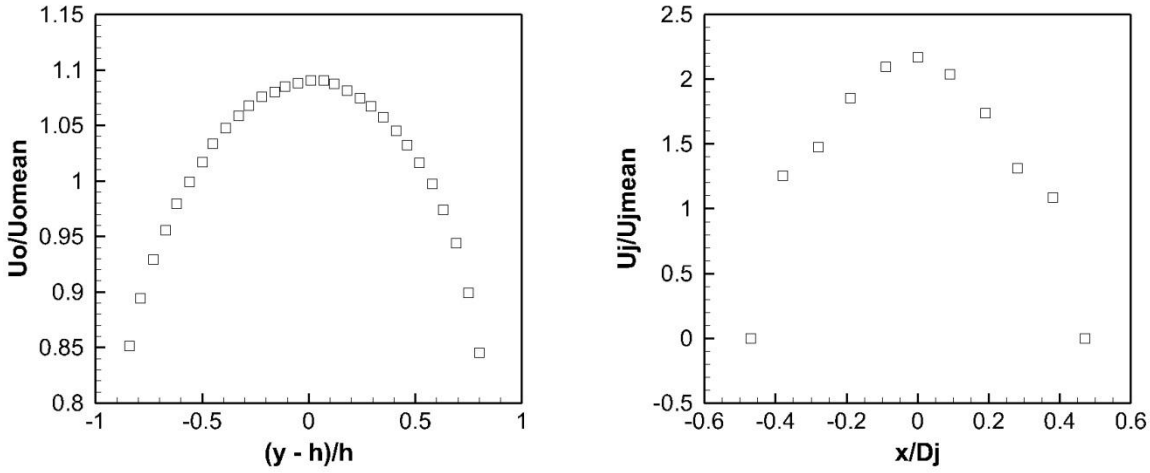

Figure 4. Initial conditions for the a) crossflow and b) jet at J = 0.075.

The interaction between the jet and crossflow was studied using particle image velocimetry (PIV). A Litron LDY 300 PIV, Nd:YLF laser was used as the light source. All images were captured using 100 ns pulses, approximately 0.5 mJ/pulse, a 120 μs time separation between pulses, and a 3348 Hz image pair capture rate. The 527 nm line of the laser was used to generate the light sheet. Due to a high level of reflections at the jet exit, the laser was operated at a reduced power level. The power difference between the laser heads when operated at the lower power level remained below 5%. Reflections were still evident however from the steel jet tube. A small reflection-induced bias toward zero displacement can be seen in Fig. 4, in the velocity profile of the jet at approximately $x/D_j = \pm 0.3$ from the center of the jet.

A Phantom V7.1 CMOS high-speed camera and the laser were synchronized using a LaVision High Speed Controller. Image pairs were processed using the LaVision DaVis 8.0.7 PIV software. A multi-pass algorithm was implemented using decreasing interrogation regions on subsequent passes. A total of four passes were completed for every image pair, two for each window size, 64 x 64 px and 32 x 32 px. Vectors with cross-correlation peak ratios $Q < 1.7$ were eliminated and replaced with a vector whose value was interpolated by using values of its nearest neighbors.

III. Results and Discussion

A total of five momentum flux ratios were studied; $J = 0.075$, 0.034, 0.014, 0.0050, and 0.0013. In terms of flow visualization, only three cases were chosen to have distinct jet and crossflow interaction. These three cases are the focus of the visualizations presented in this section. The case with maximum penetration is presented in Fig. 5, $J = 0.075$. Here the vorticity contours can be seen with respect to the instantaneous velocity field. At this instant in time, there are clear vortical structures at the leading edge of the jet and weaker vortices downstream of the

jet. Once deflected, jet fluid is forced toward the near wall and then slightly redirected into the crossflow once again.

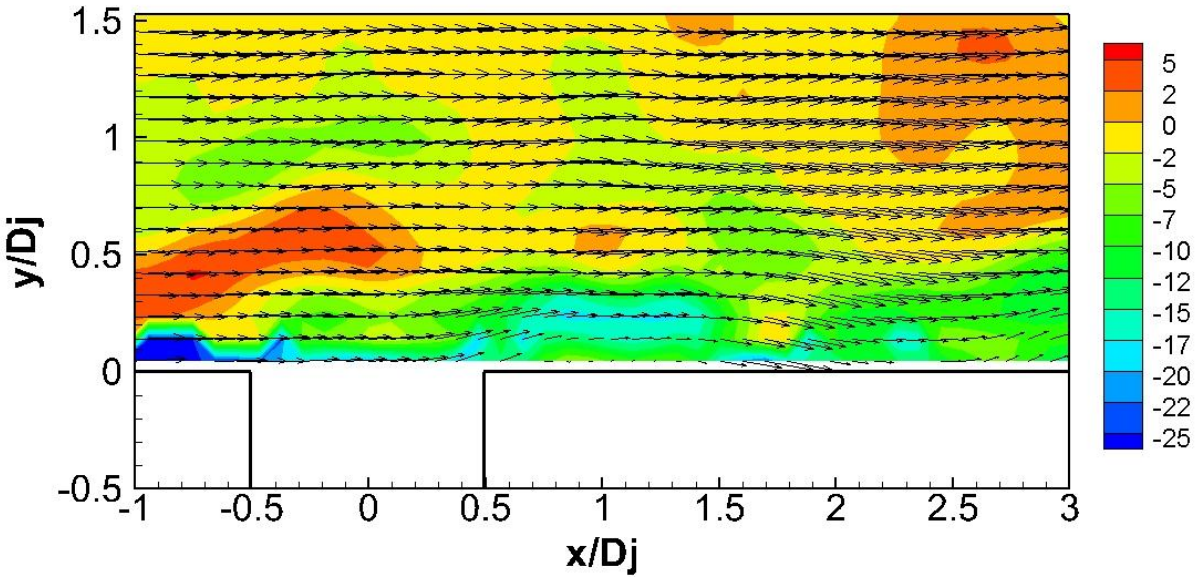

Figure 5. Vorticity contour overlaid on instantaneous vector field for J = 0.075.

Fig. 6 further illustrates this effect and shows how the mean field behavior of the jet differs as a function of the momentum flux ratio. The streamlines in Fig. 6 clearly indicate a recirculation zone downstream of the jet when J = 0.075. The lack of PIV resolution within 1 mm of the near wall does not capture what in the instantaneous field seems to be ingestion on the upstream edge of the jet. The jet fluid is constrained almost entirely to the downstream half of the jet exit, $x > 0$. The streamlines for J = 0.014 suggest the jet fluid is being constrained to the same downstream half of the jet exit, just as in the J = 0.075 case, but does not penetrate into the crossflow as much and lacks the recirculation zone visible in Fig. 6 a). When J = 0.013, the lowest value of J studied, the streamlines indicate nearly zero penetration. A slight curvature in the streamlines is seen over the entire jet exit.

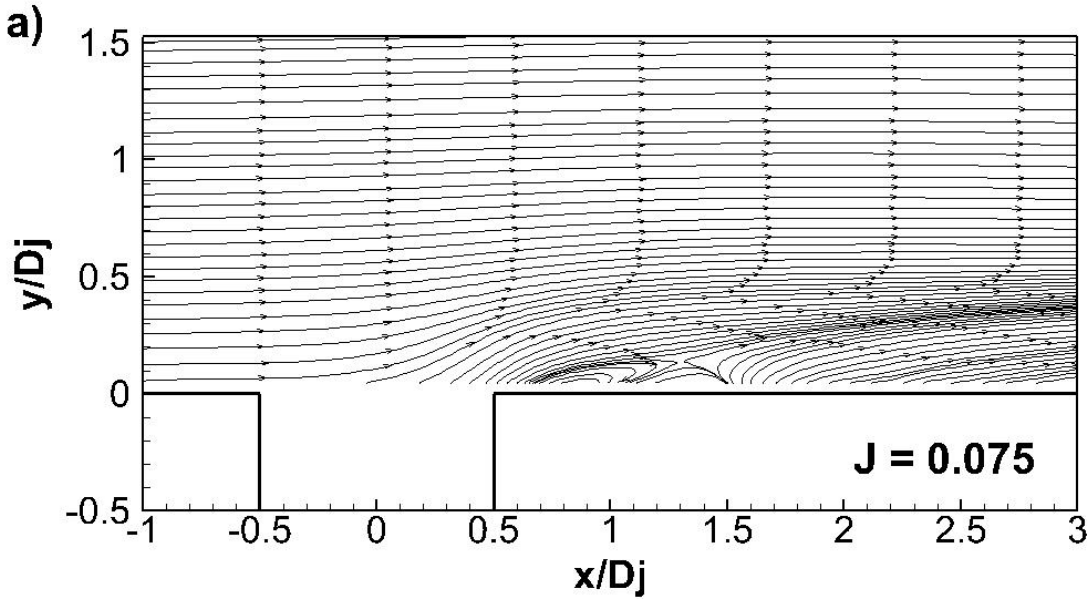

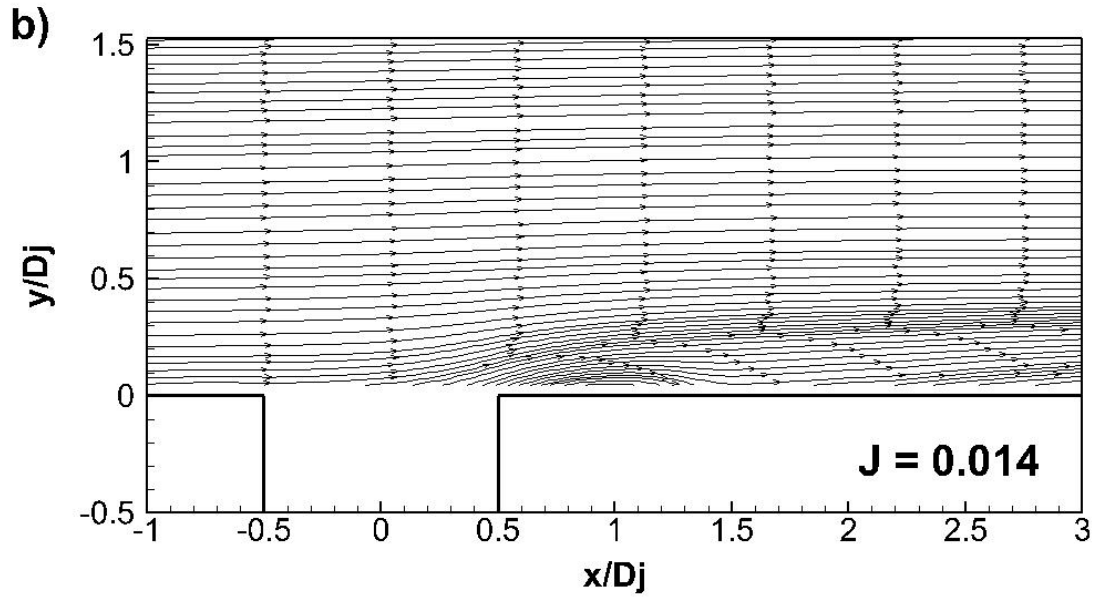

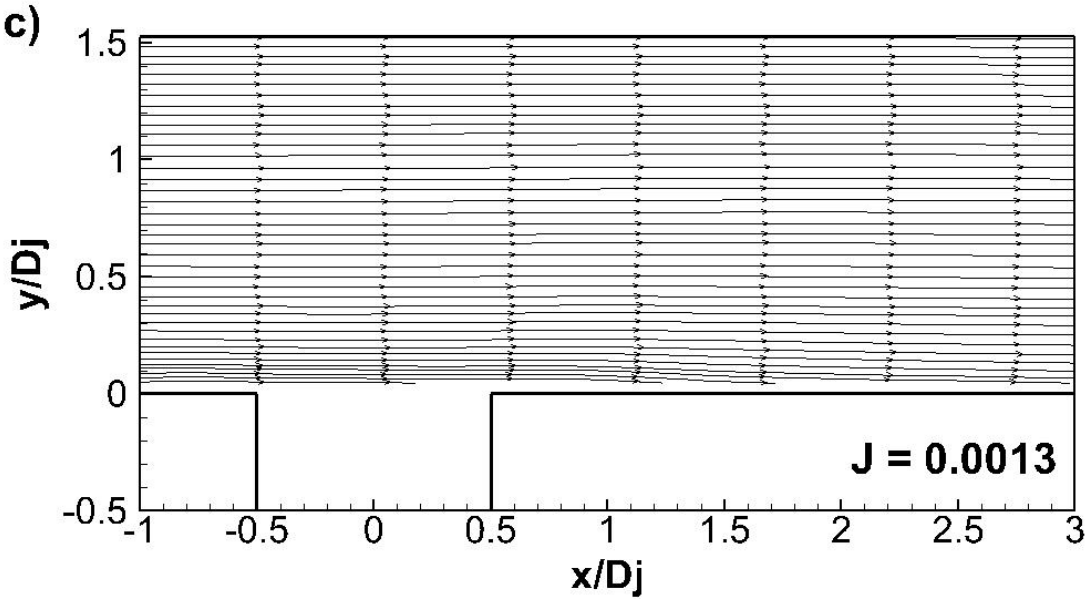

Figure 6. Streamlines of the mean velocity field for J = a) 0.075, b) 0.014, and c) 0.0013.

Fig. 7 shows that when normalized by the mean velocity of the jet, the range of momentum flux ratios investigated seem to capture a transition to a more complex 3-dimensional interaction between the jet and crossflow. When $J = 0.0050$, but especially when $J = 0.0013$, there is a negative mean velocity at the upstream edge of the jet. After returning to a nearly zero but positive velocity, the jet exhibits again a negative velocity. This behavior indicates possible ingestion on the downstream half of the jet. This and the fact that the maximum normalized-velocity of the jet never exceeds $0.9v_{mean}$, provides evidence for a complicated 3-dimensional structure which forces jet fluid to the spanwise (z-axis) perimeter of the jet. Fig. 7 b) shows the fluctuations of the instantaneous vector fields and indicates the suggested 3-dimensional jet and crossflow interaction is much more unstable than all the other cases. The data presented in Fig. 7 provides further evidence for the ingestion of crossflow fluid that is occurring on the leading edge of the jet. The crossflow fluid is penetrating into the jet hole and reducing the effective area through which the jet fluid is allowed to exit into the crossflow.

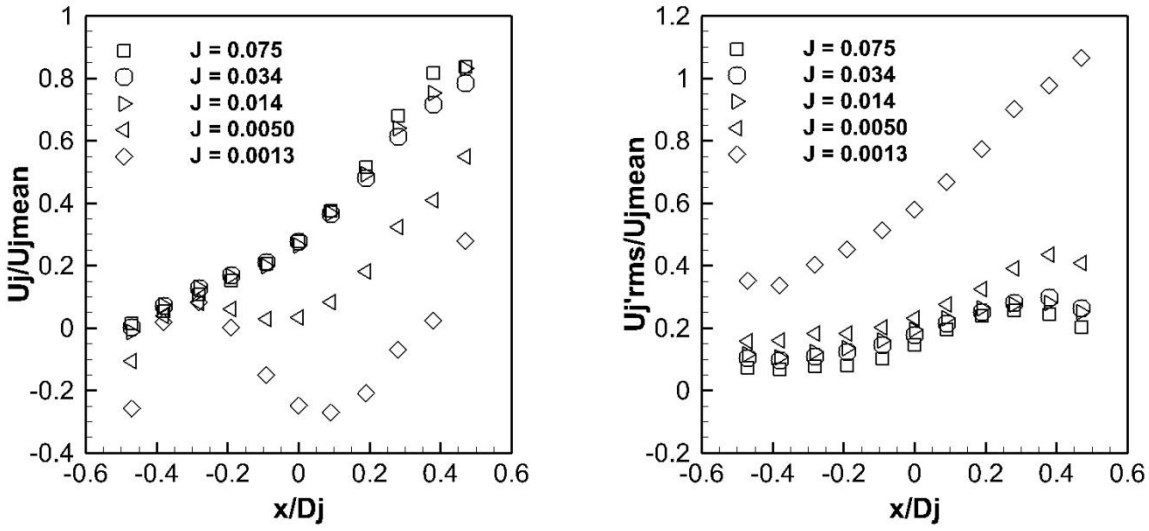

Figure 7. Jet exit a) velocity profile and b) $u_{j_{rms}}'$ profile normalized by the mean velocity of the jet, $\bar{u}_j$.

Due to the difficulty in distinguishing between crossflow and jet fluid at the jet exit, the maximum penetration values in Fig. 8 are a conservative measure of the jet's penetration into the crossflow. Maximum penetration was measured by following the streamline closest to the near wall and recording the *y* value at $x/D_j = 3$. As discussed above, there is a highly complex 3-dimensional interaction between the jet and crossflow which appears to limit the jet penetration to less than $x/D_j = 0.1$, for the two lowest *J* values. Although the fluctuations in velocity relative to the mean velocity are much greater for the lowest *J* value, it provides for minimized penetration into the crossflow. It is important to reiterate that an assumption was made about the maximum penetration occurring at the centerline of the jet, $z = 0$. With evidence for such a complex jet and crossflow interaction, it is unclear whether this assumption still holds. Future work will aim to capture velocity profiles at various *x*-*y* planes along the *z*-axis.

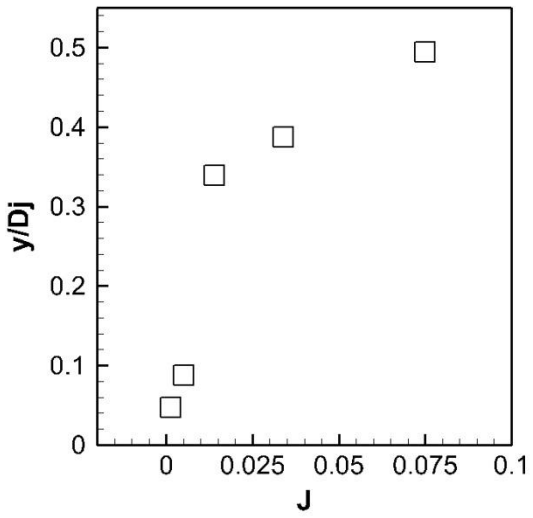

Figure 8. Maximum jet penetration.

To provide further detail on how the jet fluid is interacting with the crossflow, Fig. 9 contains Reynolds shear stress field data for the highest, middle, and lowest *J* values. Reynolds shear stress decreases directly above the jet for each subsequent decreasing value of *J*. The same trend is visible in the wake of the jet. The highest Reynolds shear stress values are found approximately three jet diameters $x/D_j = 3$, downstream of the jet exit. This occurs when $J = 0.075$.

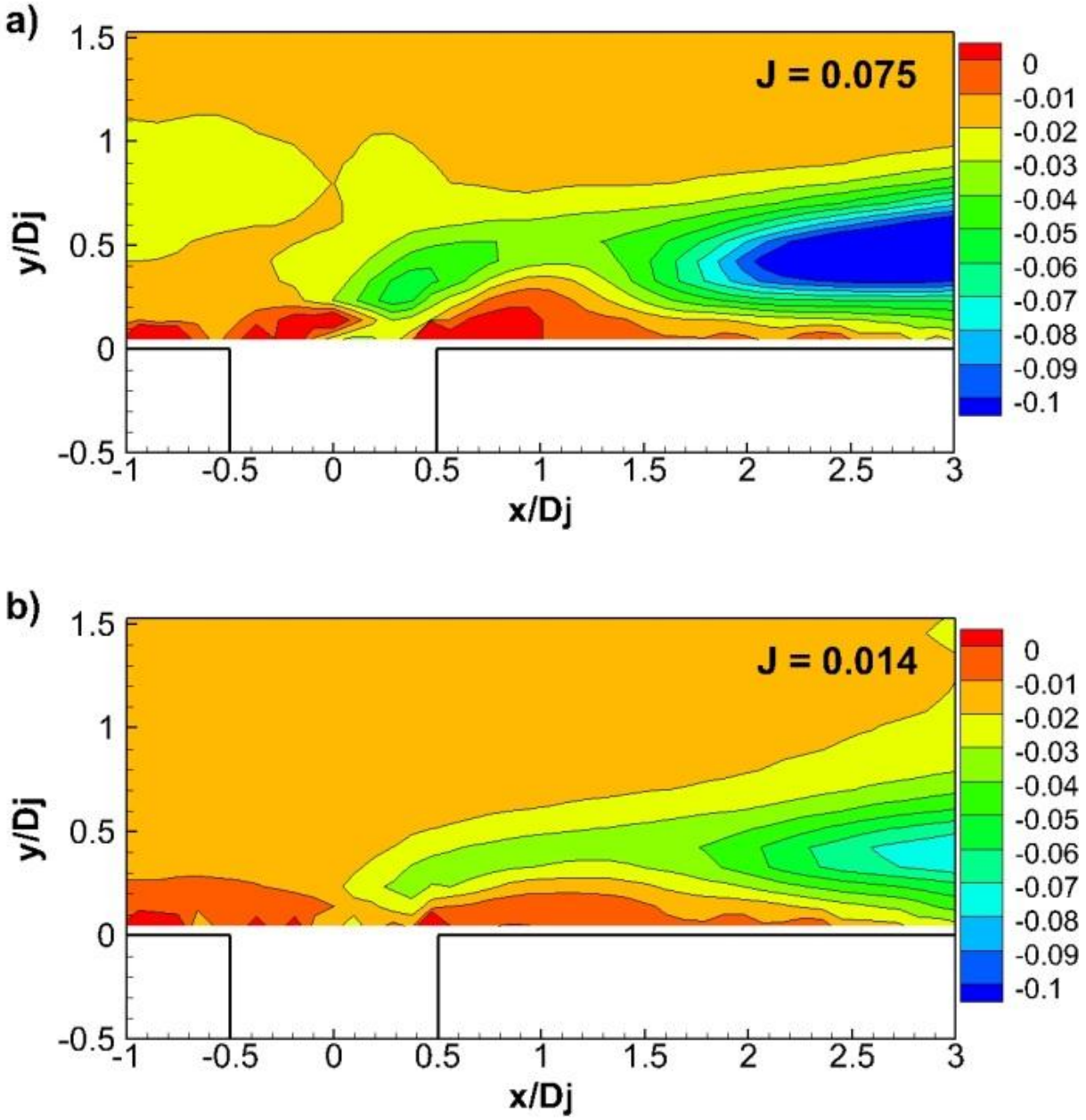

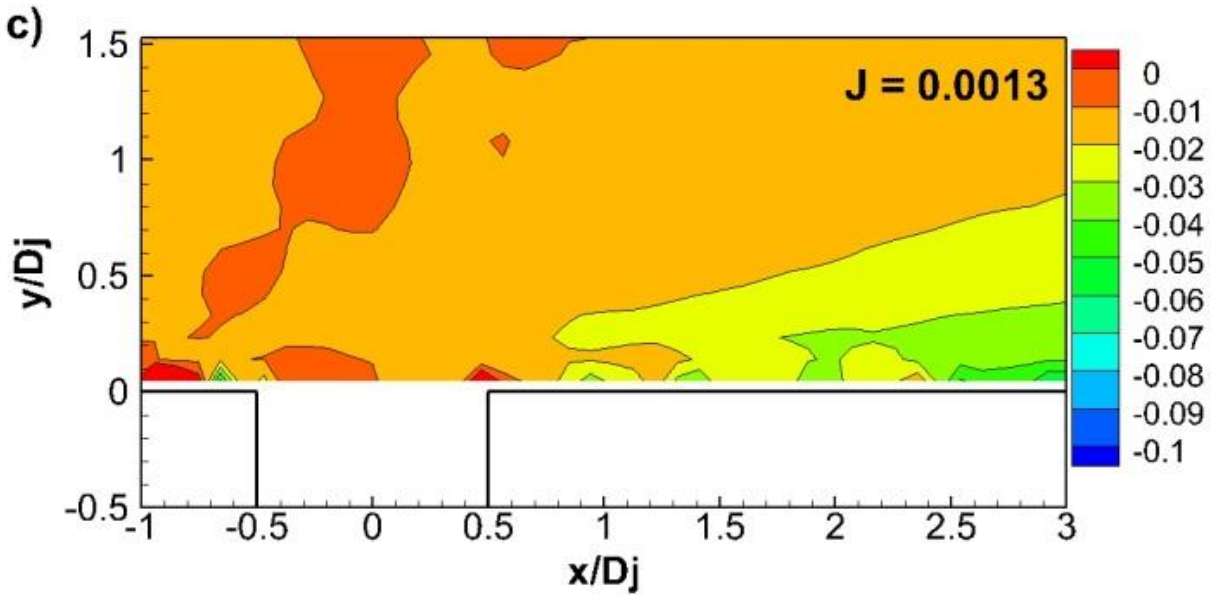

Figure 9. $\overline{u'v'}$ field for *J* = a) 0.075, b) 0.014, and c) 0.0013.

An interesting trend, which agrees with the transition from the steady and nearly 2-dimensional interaction to a more complex and 3-dimensional jet and crossflow interaction, is apparent in Fig. 10. For the highest and middle *J* values the Reynolds shear stress is constrained to approximately $0 \leq y/D_j \leq 1$. The two cases differ in that the Reynolds shear stress for the highest value of *J* is doubled as the jet convects downstream at $x/D_j = 2$ and 3. The weakest jet however, exhibits very low values of Reynolds shear stress. Despite the high levels of fluctuation, the pulsing nature of this very low case may be ideal for film cooling applications.

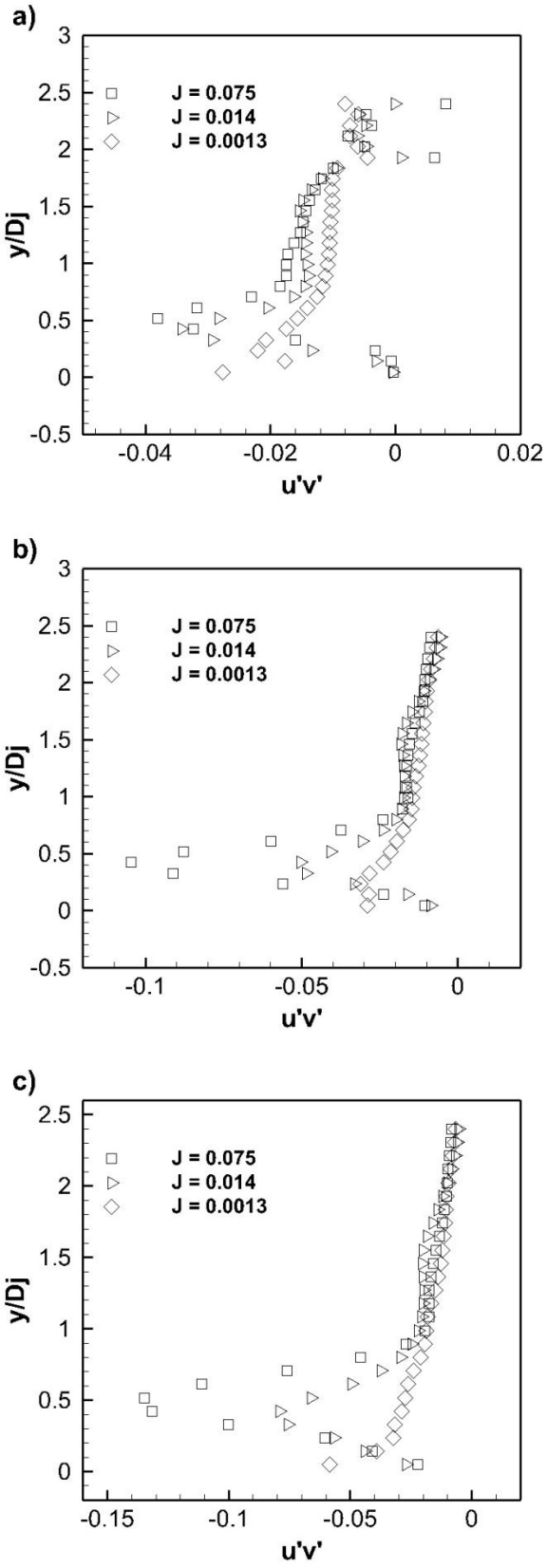

Figure 10. $\overline{u'v'}$ profiles downstream of injection at x/D_j = a) 1, b) 2, and c) 3.

A fast Fourier transform (FFT) was implemented to gain understanding on the spectral characteristics of the jet. The mean of the jet exit velocity profile, $v_{prfofile,mean}$, was calculated versus time. $v_{prfofile,mean}$ was calculated for each of the 3,000 instantaneous velocity fields. The fluctuation of the jet over time can be seen in Fig. 11 a). These fluctuations correspond to J = 0.0050. This particular case showed the highest levels of fluctuation. The frequency with the largest magnitude for each value of J is plotted in Fig. 11 b). The spectra from which these frequencies were taken are shown for three cases in Fig.12. It is clear from the spectra in Fig. 12 a) that the maximum frequency is in fact f_{max} = 1.64 Hz. This is not the case for spectra shown in Fig. 12 b). The maximum frequency for this value of J is not as easily identifiable. There appears to be other competing frequencies. Fig. 12 c) shows a prominent peak at a much larger frequency than any of the other J values.

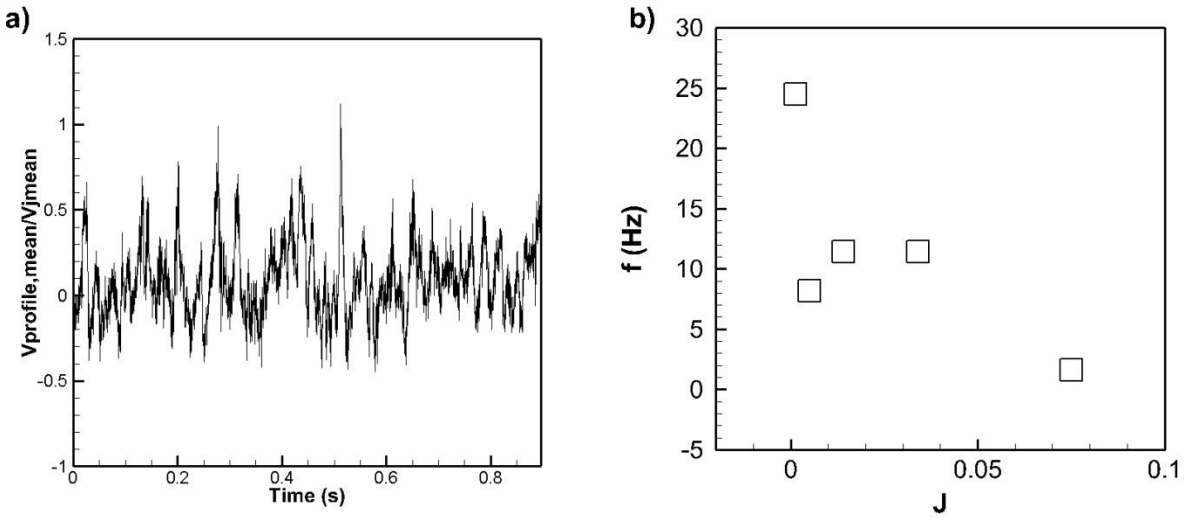

Figure 11. Mean of $v_{prfofile,mean}$ for a) J = 0.0050 and b) maximum-amplitude frequency for all values of J.

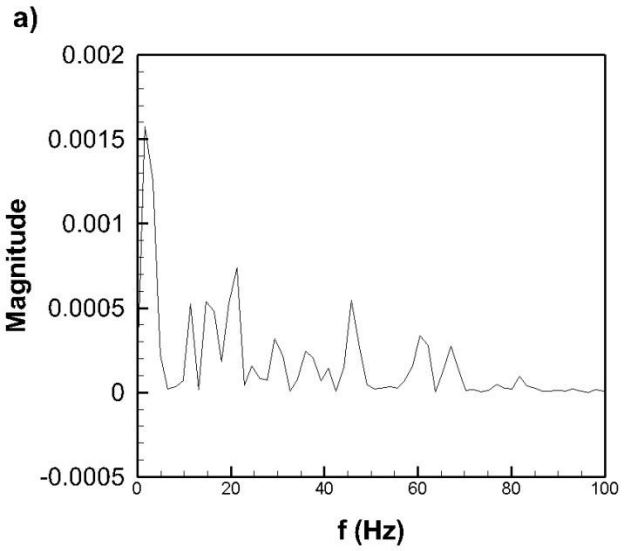

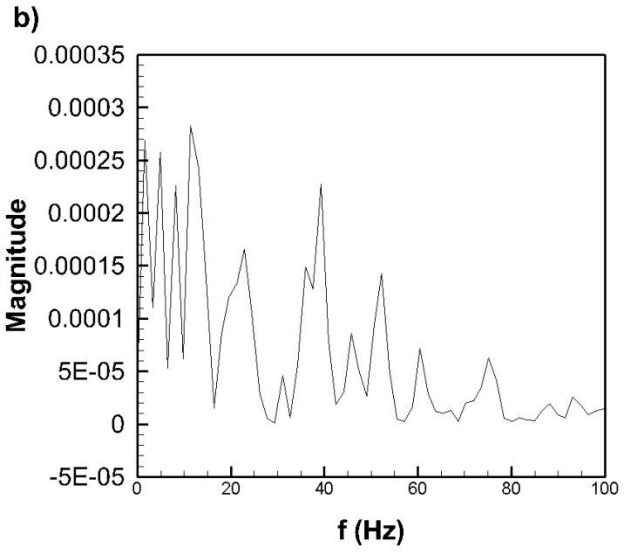

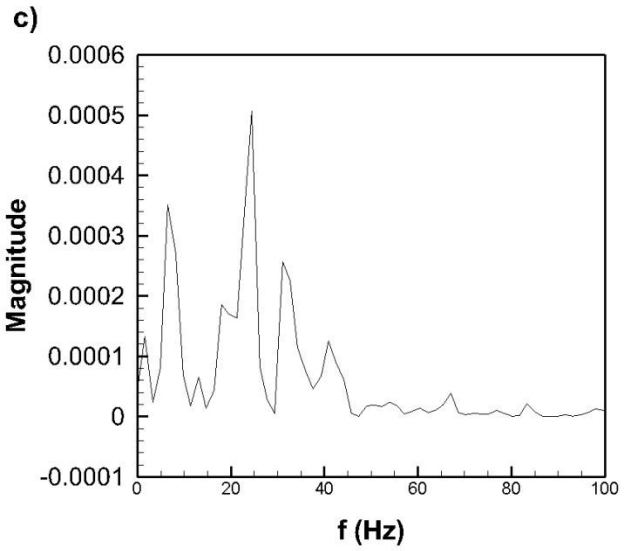

Figure 12. Jet exit velocity profile mean fluctuation-spectra for *J* = a) 0.075, b) 0.014, and c) 0.0013.

Time resolved video of all the jet cases shows how the pulse-like behavior of the jets originates from the buildup of jet fluid within the jet hole. Crossflow fluid is ingested and creates a blockage inside the jet hole. This is especially true for the $J = 0.0050$ case. For short periods of time, jet fluid is entirely prevented from exiting the jet. Jet fluid is then released after a buildup of jet fluid within the jet hole. In the $J = 0.075$ case, jet fluid is allowed to exit continuously but appears to be throttled by the buildup and release of jet fluid. The buildup and release for $J = 0.0050$ is demonstrated in Fig. 13. The jet releases zero jet fluid and in fact is ingesting crossfluid at $t = 0.193$ s. After a short period of time, jet fluid begins to penetrate into the crossflow as a very thin sheet, the built up fluid is released and penetrates nearly $1.5D_j$ into the crossflow at $t = 0.213$ s. It is interesting to note how this extended penetration into the crossflow is being convected downstream in Fig. 13 a) from an earlier discharge of jet fluid. The localized region of jet fluid that appears in Figure 13 b) convects downstream at a velocity of 1.99 m/s. This indicates that this higher region of transverse velocity is due entirely to the pulse like behavior of the jet. Future work will resolve the spectral characteristics of the jet in more detail and at other spatial locations.

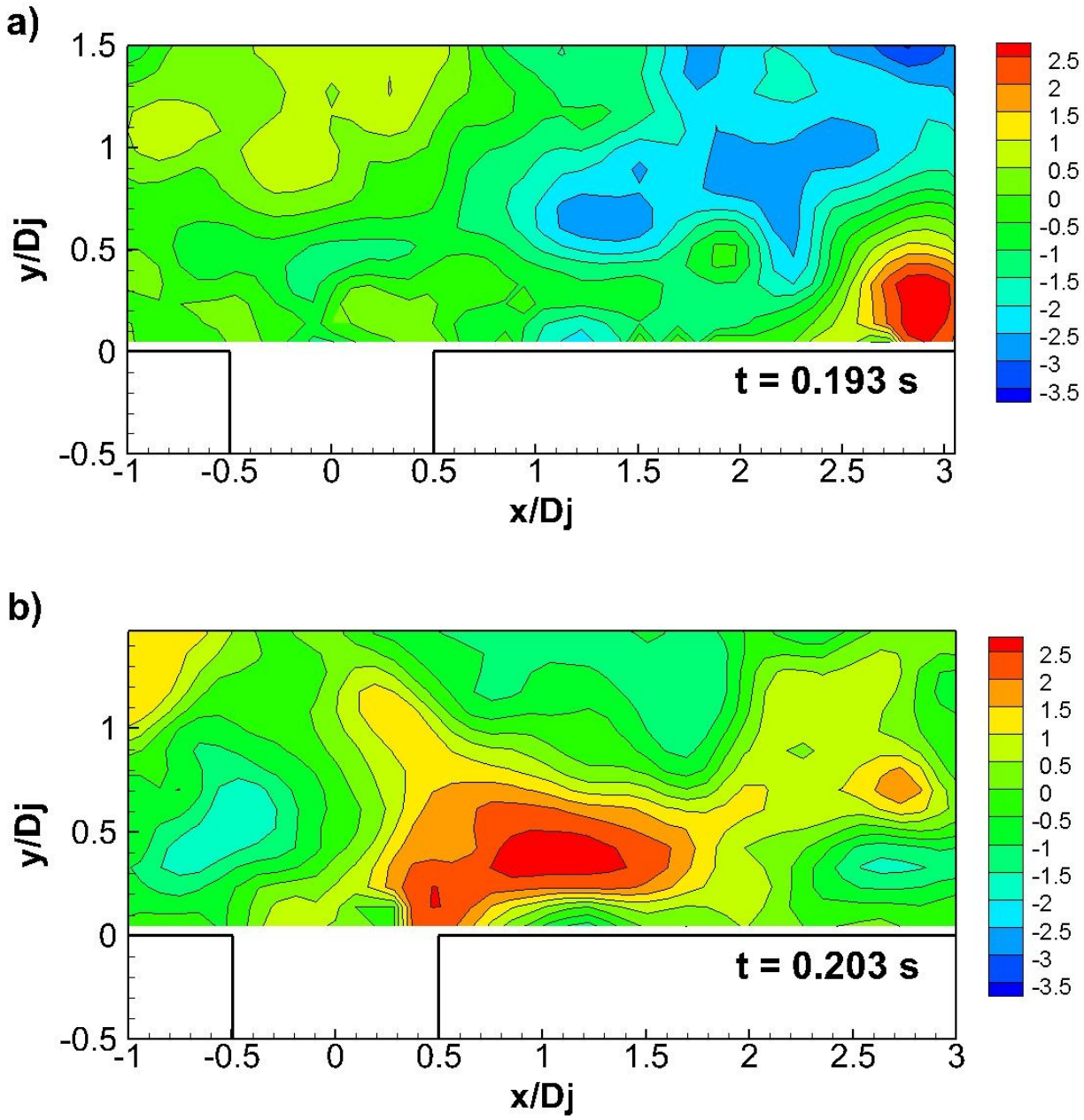

Figure 13. Time resolved pulse-like jet behavior for J = 0.0050 at t = a) 0.193 s and b) 0.203 s. Contours indicate transverse field velocity, v, normalized by the mean jet velocity, $\overline{u_j}$.

IV. Conclusion

Results generated in this study confirm jet behavior demonstrated in the research literature. For blowing ratio values $M < 0.275$, there is no visible separation or detachment of the jet from the near wall. When $J = 0.0013$, penetration is minimized. Uncertainty measurements in the MAET technique being developed at AFRL, could potentially be reduced due to the minimized penetration into the crossflow. What remains unknown however, is the structure and extent of crossflow fluid within the jet hole. Moreover, due to the high fluctuating nature of the lower value jets, MAET measurements should be taken over a time span of at least 0.90 s. This will provide the same mean jet behavior observed in the present study since this is the minimum amount of time needed (3,000 images) to capture the jet's mean behavior.

Acknowledgements

The authors of this paper thank Mr. Nils Sedano and Mr. John Stephens of AFRL's Combustion Devices Branch for their support and patience in organizing this study.

References

[1]Jenkins, T. P., and Hanson, R. K., "Soot Diagnostic for Pulse Detonation Engine Studies," *AIAA/ASME/SAE/ASEE 36th Joint Propulsion Conference*, 2000.

[2]Jenkins, T. P., and Hanson, R. K., "Soot Pyrometry Using Modulated Absorption/Emission," *Combustion and Flame*, Vol. 126, No. 3, 2001, pp. 1669-1679.

[3]Coy, E., "Demonstration of the Modulated Absorption-Emission Thermometry Technique at Conditions Simulative of a Liquid Rocket Engine Thrust Chamber," Public Affairs Clearance Number 13397, Air Force Research Laboratory, Edwards Air Force Base, CA, 2013.

[4]Sroka, L. M., and Forney, L. J., "Fluid Mixing with a Pipeline Tee: Theory and Experiment," *American Institute of Chemical Engineers*, Vol. 35, No. 3, 1989, pp. 406-414.

[5]Vranos, A., Liscinsky, D.S., True, B., and Holdeman, J.D., "Experimental Study of Cross-Stream Mixing in a Cylindrical Duct," *AIAA/SAE/ASME/ASEE 27th Joint Propulsion Conference*, 1991.

[6]Kuzo, D. M., "An Experimental Study of the Turbulent Transverse Jet," Ph.D. Thesis, California Institute of Technology, Pasadena, CA, 1996.

[7]Holdeman, J. D., Liscinsky, D. S., Oechsle, V. L., Samuelsen, G. S., and Smith, C. E., "Mixing of Multiple Jets with a Confined Subsonic Crossflow: Part I – Cylindrical Duct," *Journal of Engineering for Gas Turbines and Power*, Vol. 119, No. 4, 1997, pp. 852-862.

[8]Blomeyer, M., Krautkremer, B., Hennecke, D. K., and Doerr, T., "Mixing Zone Optimization of a Rich-Burn/Quick-Mix/Lean-Burn Combustor," *Journal of Propulsion and Power*, Vol. 15, No. 2, 1999, pp. 288-295.

[9]Leong, M. Y., Samuelsen, G. S., and Holdeman, J. D., "Optimization of Jet Mixing into a Rich, Reacting Crossflow," *Journal of Propulsion and Power*, Vol. 16, No. 5, 2000, pp. 729-735.

[10]Peterson, S. D., and Plesniak, M. W., "Evolution of Jets Emanating From Short Holes Into Crossflow," *Journal of Fluid Mechanics*, Vol. 503, 2004, pp. 57-91.

[11]Shan, J. W., and Dimotakis, P. E., "Reynolds-Number Effects and Anisotropy in Transverse-Jet Mixing," *Journal of Fluid Mechanics*, Vol. 566, 2006, pp. 47-96.

[12] Strzelecki, A., Gajan, P., Gicquel, L., and Michel, B., "Experimental Investigation of the Jets in Crossflow: Nonswirling Flow Case," *AIAA Journal*, Vol. 47, No. 5, 2009, pp. 1079-1089.

[13]Cárdenas, C., Denev, J. A., Suntz, R., Bockhorn, H., "Study of Parameters and Entrainment of a Jet in Cross-Flow Arrangement with Transition at Two Low Reynolds Numbers," *Experiments in Fluids*, Vol. 53, No. 4, 2012, pp. 965-987.

[14]Getsinger, D. R., "Shear Layer Instabilities and Mixing in Variable Density Transverse Jet Flows," Ph.D. Thesis, University of California Los Angeles, CA, 2012.

[15]Warner, C.F., and Reese, B. A., "Investigation of the Factors Affecting the Attachment of a Liquid Film to a Solid Surface," *Journal of Jet Propulsion,* Vol. 27, No. 8, 1957, pp. 877-881.

[16]Goldstein, R.J., and Eckert, E.R.G., "Effects of Hole Geometry and Density on Three-Dimensional Film Cooling," *International Journal of Heat and Mass Transfer,* Vol. 17, No. 5, 1974, pp. 595-607.

[17]Thole, K., Gritsch, M., Schulz, A., and Wittig, S., "Flowfield Measurements for Film-Cooling Holes with Expanded Exits," *Journal of Turbomachinery,* Vol. 120, No. 2, 1998, pp. 327-336.

[18]Peterson, S.D., and Plesniak, M.W., "Short-Hole Jet-in-Crossflow Velocity Field and its Relationship to Film-Cooling Performance," *Experiments in Fluids,* Vol. 33, No. 6, 2002, pp.889-898.

[19]Bidan, G., and Nikitopoulos, D.E., "On Steady and Pulsed Low-Blowing-Ratio Transverse Jets," *Journal of Fluid Mechanics,* Vol. 714, 2013, pp. 393-433.